Astron. Astrophys. 347, 69–76 (1999)

ASTRONOMY
AND
ASTROPHYSICS

Early-type stars in the Galactic halo from the Palomar–Green Survey*

II: A sample of distant, apparently young Population I stars

W.R.J. Rolleston[1], **N.C. Hambly**[2], **F.P. Keenan**[1], **P.L. Dufton**[1], **and R.A. Saffer**[3]

[1] Department of Pure and Applied Physics, The Queen's University of Belfast, Belfast BT7 1NN, Northern Ireland, UK (R.Rolleston@qub.ac.uk)
[2] Royal Observatory, Blackford Hill, Edinburgh, EH9 3HJ, Scotland (N.Hambly@roe.ac.uk)
[3] Department of Astronomy and Astrophysics, Villanova University, 800 Lancaster Avenue, PA 19085, USA (saffer@ast.vill.edu)

Received 8 December 1998 / Accepted 17 February 1999

Abstract. We present échelle (R∼40 000) spectroscopic observations for a sample of apparently normal, high Galactic latitude, early-type stars drawn from the Palomar-Green Survey. The metal-line spectra show evidence for rotational velocity broadening with values of $v \sin i \leq 300$ km s^{-1}. In conjunction with Kurucz model atmospheres, we derive stellar photospheric abundances that are consistent with a Population I chemical composition; differential abundances with respect to Galactic disk Population I stars indicate no abundance differences outside the estimated errors. From a comparison of the derived atmospheric parameters with recent theoretical evolutionary models, we derive distance and age estimates for individual stars. Using kinematical considerations, we conclude that all these objects are 'runaway' stars, formed in the Galactic disk and subsequently ejected, possibly by supernovae explosions or dynamical interactions.

Key words: stars: abundances – stars: atmospheres – stars: early-type – stars: kinematics

1. Introduction

In a previous paper (Saffer et al. 1997), we have presented low-resolution optical spectroscopy for a complete sample of blue stellar objects that have been taken from the Palomar-Green ultraviolet excess survey (Green et al. 1986). This sample represents the largest that has been obtained to date, in an attempt to resolve a number of key questions concerning the nature and origin of the faint, blue stars that are observed at intermediate and high Galactic latitudes (see Keenan 1992, for a review). Most are at a post main-sequence evolution stage, viz. white dwarfs (Bergeron et al. 1994), hot subdwarfs or extended horizontal-branch stars (Saffer et al. 1994; Hambly et al. 1997, hereafter Paper I) or post-asymptotic giant branch stars (McCausland et al. 1992). In addition, there exists a small subset of objects that are spectroscopically indistinguishable from normal, young Population I B-type stars found in the Galactic disk (Conlon et al. 1992). The majority of this subset are plausible 'runaway' stars, recently formed in the Galactic disk and subsequently ejected by some mechanism (see Leonard & Duncan 1988). However, in a few cases such as PHL 346 (Keenan et al. 1986), these apparently normal stars are found at large distances from the Galactic disk, and their evolutionary ages are too short for the objects to have attained their current Galactic locations, even given the estimated uncertainty in deriving those quantities (Ryans et al. 1996).

There is no doubt that star formation at large distances from the Galactic plane is a controversial idea. Many objects that were originally identified as distant, young halo formation candidates on the basis of low- or intermediate-resolution optical spectra, have subsequently been shown to belong to one or other of the classes of evolved, low-mass stars (see, for example, PG 0832+676, Brown et al. 1989; Hambly et al. 1996b). On the other hand, there is a certain amount of observational evidence for the existence of young stars and associations in lower gas density environments. For example, young associations of massive stars have been discovered in the 'bridge' of material between the Magellanic Clouds (Irwin et al. 1985) and model-atmosphere analyses of individual objects have confirmed their evolutionary status (Hambly et al. 1994; Rolleston et al. 1998). Also, the high Galactic latitude, young, open cluster, Blanco 1, around Zeta Sculptoris (Blanco 1949) was probably formed as a result of shocks produced during the collision of an infalling halo high-velocity cloud (HVC) with the disk interstellar medium (Edvardsson et al. 1995). Shock induced star formation between halo HVCs has been postulated as the origin of the apparently young, distant B-type stars (Dyson & Hartquist 1983) where formation *in situ* seems to be the only possible explanation for their existence.

Previously, intermediate dispersion spectroscopy of a magnitude limited sample in an equatorial survey of limited solid angle (325 square degrees), suggested that there may be as many as several hundreds of these anomalous young stars present in the Galactic halo (Hambly et al. 1993; Little et al. 1995). More recently, Rolleston et al. (1997) reported results from an on–

Send offprint requests to: W.R.J. Rolleston

* Tables 4 and 5 are only available in electronic form at the CDS via anonymous ftp to cdsarc.u-strasbg.fr (130.79.128.5) or via http://cdsweb.u-strasbg.fr/Abstract.html

Table 1. Observational details of the programme stars.

Name	Other Id.	$B_{\rm pg}$	V	y	$(b-y)$	m_1	c_1	Ref
PG 0009+036	PHL 2726	12.27	...	13.155	−0.048	0.099	0.458	1,2
PG 0855+294	CBS 29	10.34	...	12.006	−0.110	0.151	0.141	1,3
PG 0914+001	...	14.77	14.54	14.583	−0.065	0.101	0.730	1,3
PG 0934+145	...	13.23	...	13.507	−0.048	0.083	0.347	1,2
PG 0955+291	...	12.68	...	13.010	−0.053	0.090	0.594	1,3
PG 1205+228	HO+23 B	9.85	11.01	11.033	−0.081	0.111	0.309	1,4
PG 2219+094	...	9.41	...	11.915	−0.055	0.110	0.213	1,5
PG 2229+099		12.61	...	13.260	−0.011	0.073	0.288	1,2
PG 2345+241	...	11.58	12.43	12.463	−0.037	0.063	0.249	1,2,3,6

References: (1) Green et al. (1986); (2) Wesemael et al. (1992); (3) this paper; (4) Tobin (1986); (5) Moehler et al. (1990); (6) Allard et al. (1994).

going Southern hemisphere survey for 25 high-latitude stars identified as having B-type spectra. Model-atmosphere analyses of the high-resolution optical spectroscopy confirm a Population I status for 17 objects. However, to date, no object in this sample has been identified that cannot be explained as a Galactic disk runaway. In this paper, we present high-resolution optical spectroscopy of a new sample of distant, apparently young B-type stars identified from the Palomar–Green Survey. A detailed model-atmosphere/ kinematical analysis has been undertaken in an attempt to elucidate the evolutionary history of each object.

2. Observations and data reductions

2.1. Strömgren photometry

Strömgren photometry (used in the determination of stellar effective temperatures) was not available for several of the low gravity stars from the Saffer et al. (1997) sample. Observations were made using the 1.0-m Jacobus Kapteyn Telescope (JKT) on the island of La Palma on the nights of 8$^{\rm th}$ and 9$^{\rm th}$ December 1996, and employed the *uvby* filter set along with the Tek4 CCD. As the primary standards generally used in Strömgren photometry are too bright for this system, nearby stars observed by Stetson (1991) were used to standardize the instrumental magnitudes. Three exposures were obtained for both our targets and standards in each band-pass. This led to a photometric accuracy of ∼0.01 magnitudes in all filters, and the results for PG 0855+294, PG 0914+001 and PG 0955+291 are presented in Table 1.

2.2. High-resolution spectroscopy

Programme stars for high-resolution follow-up were selected from the sample presented in Saffer et al. (1997) and are detailed in Table 1, where photometric data and references are also given. The spectroscopic data were obtained using a variety of telescopes and instruments, including the William Herschel Telescope 4.0-m + UES/ ISIS spectrographs, the Mayall 4.0-m + échelle spectrograph and the Anglo-Australian Telescope 3.9-m + UCLES spectrograph. All observations employed CCDs as detectors. Reduction of the 2-dimensional CCD images to wavelength calibrated spectra was performed using tasks within the IRAF environment (Tody 1986). Standard procedures were followed, viz. overscan correction, trimming of the data section, flat-fielding, sky subtraction, extraction of the stellar spectra and wavelength calibration. Further details of the observations and reductions appear in Paper I, to which we refer the reader.

3. Results

The methods used to derive the stellar atmospheric parameters are similar to those discussed in previous papers concerning high-latitude B-type stars (see, for example, Paper I and references therein). All theoretical results are based on the grid of line blanketed model-atmospheres of Kurucz (1991), together with radiative transfer codes to derive the atmospheric parameters and chemical compositions. A normal Population I chemical composition was assumed in the atmospheric models and this was subsequently found to be appropriate for all of the stars (see Sect. 3.2).

3.1. Atmospheric parameters

Atmospheric parameters were derived for the bright, 'normal' Population I comparison stars using the same procedures as for the programme objects. Stellar effective temperatures were primarily evaluated from the reddening free Strömgren indices using the calibration of Napiwotzki et al. (1993). In all cases, the photometric uncertainties of ≤0.01 magnitudes translated to an error of less than 1 000 K in effective temperature. Estimates of the surface gravities were then deduced by comparing computed profiles of the Balmer lines (Hγ, Hδ and Hϵ) with the extracted spectra. For three objects, viz. PG 0934+145, PG 2229+099 and PG 2345+241, it was possible to obtain a second effective temperature estimate from the Si II/ Si III ionization equilibrium. Comparison of the two methods show that the latter temperatures (see Table 2) are consistently higher than the photometrically derived temperatures (presented in Table 3) by approximately 2 000 K. The calculation of the silicon line-strengths were undertaken in a non-LTE regime (see, for example, McErlean et al. 1998) and used unblanketed model atmospheres generated with the code TLUSTY (Hubeny et al.

Table 2. Silicon ionization equilibria based on non-LTE model atmosphere calculations and a microturbulence, $\xi = 0$ km s^{-1}.

Species	λ (Å)	$12 + \log(\mathrm{Si/H})_{\mathrm{NLTE}}$ 0934+145	2229+099	2345+241
Si II	3862.60	...	...	7.43
Si II	4128.07	6.81	6.85	...
Si II	4130.89	6.67	6.89	...
Si III	4552.62	6.78	6.83	7.83
Si III	4567.82	...	...	7.35
Si III	4574.76	...	...	7.59
Mean:		6.75	6.86	7.55
Standard error:		0.07	0.03	0.21
$T_{\mathrm{eff}}/10^3$ K:		18.0	20.0	21.0

Table 3. Adopted atmospheric parameters.

Target	T_{eff} ±1000 (K)	$\log g$ ±0.2 (cm s^{-2})	ξ ±3 (km s^{-1})
PG 0914+001	12 300	3.1	2.0
HR 1149[a]	13 000	3.2	2.0
PG 0009+036	14 800	3.6	5.0
PG 0934+145	16 600	4.0	5.0
PG 0955+291	13 600	3.8	5.0
PG 1205+228	16 600	4.1	5.0
HR 5595[a]	16 400	4.2	5.0
PG 0855+294	18 100	3.8	5.0
PG 2219+094	17 900	3.6	5.0
PG 2229+099	17 600	4.0	5.0
PG 2345+241	18 800	4.2	5.0
HR 6588[a]	17 700	3.9	5.0

[a] Hambly et al. (1997).

1994). By contrast, the photometric temperature calibration was based on LTE line-blanketed models of Kurucz (1991). Hence, the systematic difference in the temperature estimates from the two methods may reflect the different treatment of line blanketing. Indeed, a comparison of the temperature-optical depth scales implied that for models with similiar structures, the effective temperature label of the unblanketed non-LTE model was typically 1500–2500 K higher than that for the Kurucz model. Here, we have adopted the photometric temperature estimates to ensure consistency with the analyses of the other programme stars. Microturbulent velocities (ξ), used in the LTE analysis of the helium and metal-line spectra, were derived for two objects (PG 2229+099 and PG 2345+241) and for all comparison stars, by adjusting this parameter so as to remove the dependence of O II or S II abundance upon line-strength (see, for example, Gies & Lambert 1992). For the remaining targets, we assumed a value of the microturbulence to be similar to that of the corresponding comparison star. The final adopted atmospheric parameters for the programme stars are presented in Table 3, where they are grouped with the appropriate comparison object from the grid presented in Paper I.

3.2. Photospheric chemical compositions

Equivalent widths for the non-diffuse helium and metal-lines were measured by normalizing regions of continuum around identified lines with low-order polynomials and then, employing the non-linear least-squares Gaussian fitting routines within the spectrum analysis package DIPSO (Howarth et al. 1994). The results are given in Tables 4 and 5 for all lines in the spectra of the target stars. These tables are not reproduced here, but can be obtained electronically by ftp from the Centre de Données Stellaire, Strasbourg (http://cdsarc.u-strasbg.fr/) or from the Astrophysics & Planetary Science Division, Queen's University of Belfast, World Wide Web Server (http://star.pst.qub.ac.uk/). Also listed are the LTE abundances derived assuming the atmospheric parameters given in Table 3. Atomic data were as discussed in Jeffery (1996); however, the choice of atomic data is not critical for the differential abundance analysis.

Mean absolute abundances (on the logarithmic scale with hydrogen $\equiv$ 12.0) and normal Population I abundance values (taken from Gies & Lambert 1992, Kilian 1994) are collected in Table 6. The effect of changing the atmospheric parameters by their error estimates (see Table 3) were considered. These affected the absolute abundance estimates by typically less than 0.2 dex, and always by less than 0.3 dex. Mean differential abundances [X/H] (where the square brackets denote the abundance of the species with respect to that in the corresponding Galactic comparison) are presented in Table 7. It should be noted that in the differential analyses, the atmospheric parameters of the relevant comparison star were derived using the same technique as for the Palomar–Green targets. Such an approach should minimize the effects of systematic errors, while errors in the adopted atomic data will also be less important.

3.3. Evolutionary parameters

Stellar masses, luminosities and evolutionary ages (T_{evol}) have been deduced from the evolutionary tracks of Claret & Gimenez (1992) using the derived atmospheric parameters listed in Table 3. Values of the visual bolometric correction have been extracted from the grids of Kurucz (1979). Given the stellar mass and bolometric luminosity, we obtained a distance estimate for individual objects using the apparent visual magnitude, the visual bolometric correction and an assumed Galactic reddening law, where $E_{B-V}(b) = 0.06\mathrm{cosec}|b| - 0.06$ (Woltjer 1975) and extinction A_V=3.2$\mathrm{E_{B-V}}$. Given the relatively large Galactic latitudes of our targets, their reddening was small and hence not a significant source of error. Stellar projected rotational velocities ($v \sin i$) were also estimated by convolving synthesised spectra with rotational broadening functions until they matched the observations. Details of these parameters are given in Table 8.

Table 6. Mean absolute LTE abundances.

		12+log(X/H) ± standard error (no. of measurements)													
Ion	Pop.I	PG 0855+294		PG 0934+145		PG 0955+291		PG 1205+228		PG 2219+094		PG 2229+099		PG 2345+241	
He I	10.98	10.91 ± 0.17	(4)	10.69 ± 0.16	(4)	11.19 ± 0.21	(2)	10.98 ± 0.27	(3)	10.95 ± 0.33	(3)	10.68 ± 0.09	(6)	10.81 ± 0.09	(6)
C II	8.22	7.96	(1)	7.64 ± 0.07	(2)	8.43	(1)	8.47	(1)	7.82	(1)	8.15 ± 0.10	(3)	8.21 ± 0.15	(3)
N II	7.78	...	...	7.74	(1)	...	...	...	...	...	...	7.94 ± 0.31	(4)	7.82 ± 0.10	(3)
O II	8.47	...	...	...	...	...	...	...	...	...	...	8.99 ± 0.06	(2)	8.96 ± 0.22	(9)
Mg II	7.45	7.26	(1)	6.81	(1)	7.45	(1)	7.20	(1)	7.16	(1)	7.10 ± 0.62	(3)	7.06	(1)
Al III	6.13	...	...	...	...	...	...	...	...	...	...	5.82	(1)	6.06 ± 0.17	(2)
Si II		...	...	6.42 ± 0.06	(2)	6.69 ± 0.13	(2)	...	...	...	...	6.41 ± 0.01	(2)	6.76	(1)
Si III	7.27	...	...	7.00	(1)	...	...	...	...	...	...	7.36	(1)	7.77 ± 0.22	(3)
S II	7.21	...	...	...	...	...	...	...	...	...	...	7.08 ± 0.34	(7)	7.03 ± 0.32	(3)
S III	6.87	...	...	...	...	...	...	...	...	...	...	...	...	7.41	(1)
Ca II		...	...	5.11	(1)	...	...	...	...	...	...	...	...	...	...
Fe III	7.36	...	...	...	...	...	...	...	...	...	...	5.63	(1)	7.24 ± 0.58	(3)

Table 7. Mean differential LTE abundances.

	[X/H] ± standard error (no. of measurements)													
Ion	PG 0855+294		PG 0934+145		PG 0955+291		PG 1205+228		PG 2219+094		PG 2229+099		PG 2345+241	
He I	$+0.09 \pm 0.21$	(2)	-0.11 ± 0.12	(4)	$+0.38 \pm 0.21$	(2)	$+0.15 \pm 0.30$	(3)	$+0.24 \pm 0.34$	(3)	-0.08 ± 0.07	(6)	$+0.05 \pm 0.06$	(6)
C II	-0.19	(1)	-0.44	(1)	$+0.30$	(1)	$+0.34$	(1)	-0.21	(1)	$+0.01 \pm 0.15$	(3)	$+0.06 \pm 0.05$	(3)
N II	...	...	$+0.09$	(1)	...	...	...	...	...	...	$+0.10 \pm 0.30$	(4)	$+0.01 \pm 0.24$	(3)
O II	...	...	...	...	...	...	...	...	...	...	$+0.13 \pm 0.06$	(2)	$+0.19 \pm 0.26$	(9)
Mg II	-0.60	(1)	-0.36	(1)	$+0.28$	(1)	$+0.03$	(1)	$+0.08$	(1)	$+0.18 \pm 0.21$	(2)	-0.02	(1)
Al III	...	...	...	...	...	...	...	...	...	...	-0.46	(1)	-0.04 ± 0.42	(2)
Si II	...	...	-0.20 ± 0.01	(2)	...	...	...	...	...	...	-0.08 ± 0.02	(2)	-0.05	(1)
Si III	...	...	...	...	...	...	...	...	...	...	-0.27	(1)	$+0.25 \pm 0.18$	(3)
S II	...	...	...	...	...	...	...	...	...	...	$+0.13 \pm 0.25$	(7)	$+0.15 \pm 0.22$	(3)
S III	...	...	...	...	...	...	...	...	...	...	...	...	$+0.42$	(1)
Ca II	...	...	...	...	...	...	...	...	...	...	...	...	...	...
Fe III	...	...	...	...	...	...	...	...	...	...	$+0.22$	(1)	$+0.25 \pm 0.34$	(3)

Table 8. Kinematic and derived evolutionary parameters.

Star	l°	b°	$v \sin i$ (km s^{-1})	Mass ($M_\odot$)	M_V	v_{lsr} (km s^{-1})	v_r (km s^{-1})	z (kpc)	T_{evol} (Myr)	T_f (Myr)	T_{evol}(MAX) (Myr)	T_f(MIN) (Myr)	v^z_{ej} (km s^{-1})
PG 0009+036	104.58	-57.57	350 ± 50	5.6	-2.006	140 ± 18	169	9.09	80	36	...	...	289
PG 0855+294	196.08	$+39.12$	110 ± 15	6.7	-2.058	58 ± 4	93	4.10	45	23	...	...	201
PG 0914+001	231.68	$+31.84$	325 ± 50	5.8	-2.950	80 ± 20	-30	16.94	79	139	...	...	293
				4.7	-1.608		16	8.44	...	...	116	70	204
PG 0934+145	218.61	$+43.08$	30 ± 8	5.3	-1.146	105 ± 4	97	5.82	61	39	...	...	192
PG 0955+291	199.88	$+51.94$	190 ± 30	4.4	-1.091	72 ± 14	58	5.20	127	41	...	...	172
PG 1205+228	235.56	$+79.12$	165 ± 17	5.1	-0.854	156 ± 4	155	2.34	51	13	...	...	187
PG 2219+094	73.16	-38.40	225 ± 20	7.5	-2.665	-17 ± 8	-7	5.12	41	67	...	...	155
				6.5	-2.229		-7	4.19	...	...	53	62	140
PG 2229+099	76.07	-39.64	16 ± 5	5.8	-1.347	-10 ± 5	5	5.32	49	61	...	...	158
				5.4	-1.303		9	5.22	...	...	63	58	157
PG 2345+241	105.05	-36.29	48 ± 9	6.0	-1.002	82 ± 3	112	2.92	19	14	...	...	221

3.4. Kinematical analysis

We have undertaken a kinematical investigation in order to determine whether these high-latitude, normal Population I objects could be 'runaway' stars – born and subsequently ejected from the known sites of star formation in the Galactic disk. Reliable proper motions are not readily available for our targets; therefore, in the first instance we have used the observed radial velocity of a star to constrain its evolutionary history. Our method of analysis is outlined briefly below; the full details can be found in Rolleston et al. (1997) and references therein.

The kinematical analysis is summarized in Table 8. Stellar radial velocities (v_{lsr}) were measured using the Doppler shifts of all lines identified in the high-resolution optical spectra, relative to the Local Standard of Rest in the solar neighbourhood. These have been transformed to a standard of rest defined by a star's local environment (v_r), by correcting for the effects of differential Galactic rotation (Fich et al. 1989) assuming that the halo co-rotates with the disk. As a first approach, we have considered the scenario whereby a star has a zero velocity component parallel to the Galactic disk, ie. its space motion is perpendicular to the plane of the Galaxy. Flight-times (T_f) have therefore been determined using the estimated stellar space velocity (v_z) perpendicular to the plane of the Galactic disk, the inferred z-distance and the gravitational potential function of House & Kilkenny (1980). Any subsequent comparison with

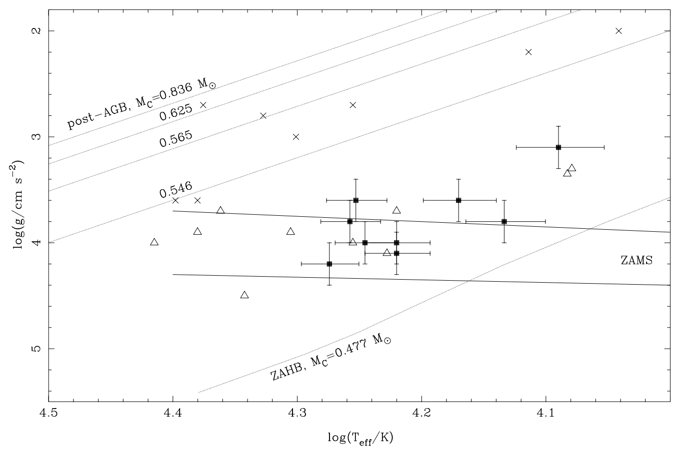

Fig. 1. The $T_{\rm eff} - \log g$ diagram for the programme objects (solid squares), where the theoretical positions of the zero-age hydrogen burning main-sequence (ZAMS), blue horizontal branch (BHB) and post-asymptotic giant branch (post-AGB) are given (Bertelli et al. 1994; Sweigart 1987; Schönberner 1993 respectively). Also shown are some candidate post-AGB stars (crosses) studied previously by us (Hambly et al. 1996a; Conlon et al. 1994; McCausland et al. 1992 and the post-BHB stars (open triangles) from the Hambly et al. (1997) PG sample (Paper I).

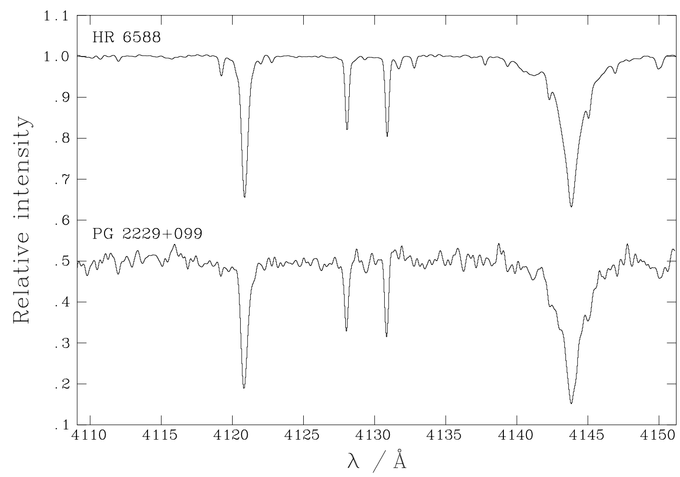

Fig. 2. Comparison between target and standard spectra

evolutionary timescales implicitly assume that the stars were ejected from the disk shortly after gravitational collapse, consistent with cluster ejection simulations (Leonard 1993).

4. Discussion

The target stars are plotted in the $T_{\rm eff} - \log g$ plane in Fig. 1, and appear to scatter above the zero-age main-sequence (ZAMS), although this diagram is of course insufficient to class the objects as young, high-mass hydrogen burning stars. However, they are unlikely to be evolved, low mass stars on the basis of their generally large projected rotational velocities; in stark contrast to the post-blue horizontal branch (post-BHB) sample presented in Paper I. In addition, the surface gravities appear to be too high for the objects to be post-asymptotic giant branch stars (post-AGB, *cf.* McCausland et al. 1992); in any case, none of the compositional peculiarities often observed in post-BHB and post-AGB stars are observed in this sample.

The similarity between the spectra of this sample and those of our Galactic disk comparision stars is illustrated in Fig. 2, where we plot sections of spectra for PG 2229+099 plus the comparison HR 6588. Once convolved with the appropriate rotational broadening function, corresponding spectra are effectively identical. The validity for using the bright Galactic disk B-type stars as standards of Population I chemical composition has been verified by the abundance values found in Paper I. From Table 7, there is no strong evidence for any departures from a Population I chemical composition in any of the PG–targets. In brief, all the available evidence points to the objects being distant young high-mass Population-I B-type stars. We now discuss each object separately:

PG 0009+036. This object (≡PHL 2726) has been analysed recently by Schmidt et al. (1996) using intermediate resolution optical and ultraviolet spectra. We find similar atmospheric parameters to that study; in addition, the diffuse helium-line spectrum infers a normal composition. Unfortunately, no other abundance information is available due to the absorption lines being washed out by the large projected rotational velocity ($v \sin i \sim 350$ kms^{-1}). PG 0009+036 is at a large Galactic latitude (of 60°) which combined with the derived stellar parameters places it ∼9 kpc below the Galactic plane. However, this object is a classic 'runaway' as it exhibits a large peculiar motion ($v_{\rm r} \sim 169$ kms^{-1}). Furthermore, the kinematical analysis shows that this star could have formed and have been subsequently ejected from the Galactic disk.

PG 0855+294. This object was originally discovered in the Case low-dispersion Northern sky survey (≡CBS 29, Sanduleak & Pesch 1984). The moderately large projected rotational velocity precludes any abundance measurements other than that for helium, carbon and magnesium which appear normal. The kinematic analysis demonstrates that this star could quite reasonably have had time to travel to its current position.

PG 0914+001. This object is potentially the most interesting in the sample as it is the faintest and yet is clearly young, due to the large projected rotational velocity ($v \sin i \sim 325$ kms^{-1}) and the presence of emission in the early Balmer lines (see Fig. 3). The latter introduces a larger uncertainty in our surface gravity estimate (∼0.3 dex), while the former leads to few absorption features being observed in the spectrum – thus making the model-atmosphere analysis difficult.

Our choice of atmospheric parameters yield a normal, photospheric helium composition of 11.0±0.3 dex. Furthermore, these imply an evolutionary age that is less than the time of flight obtained from the kinematical analysis, placing PG 0914+001 some 16.9 kpc above the Galactic plane and at a galactocentric radius ($R_{\rm g}$) of 33.2 kpc! However, it is important to consider

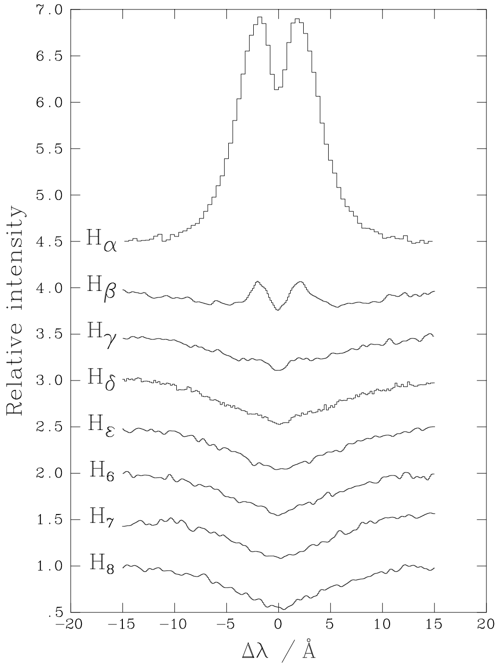

Fig. 3. Balmer series for PG 0914+001, showing emission in the earliest lines.

the effect of errors in the derived atmospheric parameters and the radial velocity – as these in turn will affect our estimates of the stellar distance and life-time. We have therefore considered a ($T_{\rm eff}$, $\log g$) pair that is consistent within our observational errors, but which will minimize the ratio of the kinematic time-of-flight to the evolutionary age. For example, the atmospheric parameters (13 000 K, 3.6 dex) lead to an evolutionary age, $T_{\rm evol}$, that is greater than the time-of-flight, $T_{\rm f}$(MIN), needed for PG 0914+001 to attain its current Galactic position and the results of this error analysis are entered as a second line in Table 8. Furthermore, this choice of ($T_{\rm eff}$, $\log g$) pair lead to more 'realistic' values of z-distance and galactocentric radius.

PG 0934+145. The available abundance estimates for this star, although somewhat discordant, are not significantly different from those of the Population I analogue. The large peculiar radial motion implies a large velocity perpendicular to and away from the Galactic plane – and is strong evidence that PG 0934+145 originated in the Galactic disk.

PG 0955+291. This object also presents a Population I chemical composition and a large projected rotational velocity. Although PG 0955+291 is at a moderatively large distance ($z \sim 5.2$ kpc) above the Galactic plane, there is no reason to suppose that it can not have travelled to its current position within its estimated lifetime, given its peculiar motion orthogonal to and away from the Galactic plane.

PG 1205+228. A model atmosphere analysis of this star (≡HO+23 B) has been presented previously (Conlon et al. 1989); in addition, a kinematic analysis appears in Conlon et al. (1990). This star is most certainly a Galactic disk runaway, at Galactic latitude $b = +79°$ and with a large positive radial velocity of 156 ± 4 km s^{-1}.

PG 2219+094. This broad-lined star ($v \sin i \sim 225$ km s^{-1}) proved difficult to analyse. However, it is clearly young and the abundance estimates for carbon and magnesium are Population I. The kinematical analysis requires flight-times that are greater than the stellar evolutionary age, despite considering the effect of errors in the derived atmospheric parameters and radial velocity measurement. Although apparently situated at a moderately large distance ($z \sim 5$ kpc) below the Galactic plane, it would be unwise to postulate halo formation as the origin, given the relatively small Galactic latitude of this star and without a much more precise measurement of the star's velocity perpendicular to the plane. Recently, Thejll et al. (1997) presented proper motion measurements for PG 2219+094 and several other PG stars in common with this paper and Paper I. These are discussed further in Sect. 5.

PG 2229+099. This sharp-lined star presents a reasonably rich metal-line spectrum and therefore has well defined abundance estimates, which show no significant deviation from a Population I chemical composition. Indeed, the observed spectrum is very similiar to that of the comparison star HR 6588 (see Fig. 2). PG 2229+099 is observed at a moderately large z-distance below the plane. However, the kinematical error analysis demonstrates that this object could have originated in the Galactic disk.

PG 2345+241. A normal metallicity was derived for this star, the moderately low projected rotational velocity permitting the reliable determination of abundance estimates for many species. PG 2345+241 is a young object, with $T_{\rm evol} \sim 19$ Myr. However, it lies a mere 2.9 kpc below the plane and has a large positive radial velocity, making it possible to attain its current Galactic location within its lifetime.

5. Proper motions

For the low Galactic latitude objects, the kinematic analysis is limited by the lack of proper motion data (eg. Rolleston et al. 1997; Heber et al. 1997). Recently, Thejll et al. (1997) presented proper motion measurements for a sample of 138 PG stars that were classified as being hot sub-dwarfs; these include four of our programme stars, viz. PG 0009+036, PG 2219+094, PG 2229+099 and PG 2345+241. The proper motion vectors (μ, θ) in the equatorial coordinate system were converted to the Galactic coordinate system ($\dot{l}$, $\dot{b}$) using the numerical routines within SLALIB (Wallace 1992). Velocity components perpendicular to, and parallel with the Galactic plane were calculated from the peculiar radial motion and proper motion. The 'true' z-velocity was then used to compute time-of-flights; details of the revised kinematical analysis are given in Table 9.

Table 9. Stellar proper motions.

Star	b°	$v_{\rm r}$ (km s^{-1})	μ (mas yr^{-1})	θ ($^{\circ}$)	$v_{\rm ej}$ (km s^{-1})
PG 0009+036	-57.57	$+169$	7.6±3.9	23±56	330–470
PG 2219+094	-38.40	-7	6.2±3.6	194±47	180–410
PG 2229+099	-39.64	$+5$	7.1±4.1	236±61	190–470
PG 2345+241	-36.29	$+112$	7.0±2.0	255±7	200–260

In particular, the proper motion of PG 2219+094 makes a significant contribution to the star's velocity perpendicular to the plane. Indeed, the revised velocity, $v_{\rm z} \sim 98$ km s^{-1}, reveals the runaway nature of this star – the subsequent kinematical analysis confirming that PG 2219+094 could have been ejected from the star-formation regions of the Galactic disk. The inclusion of the proper motion information for the other three programme stars in the kinematical analyses, support the conclusions presented in Sect. 4.

Unfortunately, the errors of measurement yield a large spread in the possible ejection velocities (see Table 9), and hence it is difficult to make any conclusion about the ejection mechanism. Moreover, these proper motions have been derived using comparisons between absolute positions on AGK3/FK5 equinox systems, and may contain relatively large systematic errors for objects that are expected to have very small proper motions (eg. of order 10 mas yr^{-1}). The problem of non-inertial pre–FK5 equinoxes is discussed in, for example, Fricke (1982) and references therein. Absolute proper motions measured with long time baseline plate pairs and with respect to galaxies may provide more accurate information (eg. the Lick Northern Proper Motion project, Klemola et al. 1987). However, the input catalogue for this project contains none of the stars discussed here, and the accuracy of the proper motions measured is ~ 5 mas yr^{-1} (Jones 1996). With the completion of the second epoch Palomar sky survey, a better approach may be to determine relative proper motions with subsequent corrections for absolute proper motions perpendicular to the Galactic disk – for the purposes of estimating velocities in the z-direction. Sky limited 48 inch Schmidt plates are not ideal for astrometry of objects brighter than m∼14 mag due to off–centred image halos as a function of plate position; this problem is compounded by the POSS-I (Minkowski & Abell 1963) and POSS-II (Reid et al. 1991) field centres being different. Despite this, a careful treatment of magnitude–dependent systematic effects coupled with a centroiding accuracy of ∼1 μm, a plate scale of ∼0.07 arcsec mm^{-1} and an epoch difference of ~ 40 yr may yield proper motions of accuracy ~ 2 mas yr^{-1} (see Hambly et al. 1998).

6. Conclusions

High resolution échelle spectroscopy of 21 stars from the complete sample presented in Saffer et al. (1997) has revealed 9 objects that appear to belong to the young Population I. Unfortunately the age of these high-mass objects implies generally large values of the stellar rotational velocity, and in all but a few cases, quantitative metal abundances are difficult to measure (in contrast with the evolved stellar sample presented in Paper I). The available kinematic information indicates that all stars, with one possible exception (viz. PG 2219+094), originated in the Galactic disk and were subsequently ejected. However, the inclusion of proper motion data for PG 2219+094 makes a significant contribution to the estimated velocity of this object perpendicular to the Galactic plane; and the evidence points to a Population I disk origin for this target also. The completion of the high-resolution spectroscopic follow-up for the Saffer et al. (1997) sample, along with *reliable* proper motion determinations, will help to answer the outstanding questions concerning the nature and origin of the anomalous young, distant blue stars in the Galactic halo.

Acknowledgements. NCH and WRJR acknowledge continuing financial support from the UK PPARC, RAS acknowledges support from the ST ScI Director's Discretionary Research Fund, and FPK acknowledges support from the Royal Society. The William Herschel and Jacobus Kapteyn Telescopes on the island of La Palma are operated by the Royal Greenwich Observatory, on behalf of the UK PPARC, at the Spanish Observatorio del Roque de los Muchachos of the Instituto de Astrofisica de Canarias. This research has made use of the SIMBAD database operated at the CDS, Strasbourg, France.

References

Allard F., Wesemael F., Fontaine G., Bergeron P., Lamontange R., 1994, AJ 107, 1565
Bergeron P., Wesemael F., Beauchamp A., et al., 1994, ApJ 432, 305
Bertelli G., Bressan A., Chiosi C., Fagatto F., Nasi E., 1994, A&AS 106, 275
Blanco V.M., 1949, PASP 61, 183
Brown P.J.F., Dufton P.L., Keenan F.P., et al., 1989, ApJ 339, 397
Claret A., Giménez A., 1992, A&AS 96, 255
Conlon E.S., Brown P.J.F., Dufton P.L., Keenan F.P., 1989, A&A 224, 65
Conlon E.S., Dufton P.L., Keenan F.P., Leonard P.J.T, 1990, A&A 236, 357
Conlon E.S., Dufton P.L., Keenan F.P., McCausland R.J.H., Holmgren D.E., 1992, ApJ 400, 273
Conlon E.S., Dufton P.L., Keenan F.P., 1994, A&A 290, 897
Dyson J.E., Hartquist T.W., 1983, MNRAS 203, 1233
Edvardsson B., Pettersson B., Kharrazi M., Westerlund B., 1995, A&A 293, 75
Fich M., Blitz L., Stark A.A., 1989, ApJ 342, 272
Fricke W., 1982, A&A 107, L13
Gies D.R., Lambert D.L., 1992, ApJ 387, 673
Green R.F., Schmidt M., Liebert J., 1986, ApJS 61, 305
Hambly N.C., Conlon E.S., Dufton P.L., et al., 1993, ApJ 417, 706
Hambly N.C., Dufton P.L., Keenan F.P., et al., 1994, A&A 285, 716
Hambly N.C., Keenan F.P., Dufton P.L., Lumsden S.L., 1996a, MNRAS 278, 811
Hambly N.C., Keenan F.P., Dufton P.L., et al., 1996b, ApJ 466, 1018
Hambly N.C., Rolleston W.R.J., Keenan F.P., Dufton P.L., Saffer R.A., 1997, ApJS 111, 419 – Paper I
Hambly N.C., Miller L., MacGillivray H.T., Herd J., Cormack W.A., 1998, MNRAS 298, 897

Heber U., Moehler S., Schmidt J.H.K., et al., 1997, In: Proceedings of the Third conference on Faint Blue stars, in press
House F., Kilkenny D., 1980, A&A 81, 251
Howarth I.D., Murray J., Mills D., 1994, Starlink User Note No. 50.15
Hubeny I., Lanz T., Jeffery C.S., 1994, TLUSTY and SYNSPEC – A Brief Description, CCP7
Irwin M.J., Kunkel W.E., Demers S., 1985, Nat 318, 160
Jeffery C.S., 1996, QJRAS 37, 39
Jones B.F., 1996, private communication
Keenan F.P., Lennon D.J., Brown P.J.F., Dufton P.L., 1986, ApJ 307, 694
Keenan F.P., 1992, QJRAS 33, 325
Kilian J., 1994, A&A 282, 867
Klemola A.R., Jones B.F., Hanson R.B., 1987, AJ 94, 501
Kurucz R.L., 1979, ApJS 40, 1
Kurucz R.L., 1991, In: Davis-Philip A.G., Upgren A.R., Janes P.L. (eds.) Precision Photometry: Astrophysics of the Galaxy 27, L. Davis Press, Schenectady
Leonard P.J.T., 1993, In: Sasselov (ed.) Luminous High-latitude Stars. ASP 45, 306
Leonard P.J.T., Duncan M.J., 1988, AJ 96, 222
Little J.E., Dufton P.L., Keenan F.P., et al., 1995, ApJ 447, 783
McCausland R.J.H., Conlon E.S., Dufton P.L., Keenan F.P., 1992, ApJ 394, 298
McErlean N.D., Lennon D.J., Dufton P.L., 1998, A&A submitted
Minkowski R.L., Abell G.O., 1963, In: Stravel K.A. (ed.) Stars and Stellar Systems, vol. III, 481
Moehler S., Richtler T., de Boer K.S., Dettmar R.J., Heber U., 1990, A&AS 86, 53
Napiwotzki R., Schönberner D., Wenkse V., 1993, A&A 268, 653
Reid I.N., Brewer C., Brucato R.J., et al., 1991, PASP 103, 661
Rolleston W.R.J., Hambly N.C., Dufton P.L., et al., 1997, MNRAS 290, 422
Rolleston W.R.J., Dufton P.L., McErlean N.D., Venn K.A., 1998, A&A, submitted
Ryans R.S.I., Hambly N.C., Dufton P.L., Keenan F.P., 1996, MNRAS 278, 132
Saffer R.A., Bergeron P., Koester D., Liebert J., 1994, ApJ 432, 351
Saffer R.A., Keenan F.P., Hambly N.C., Dufton P.L., Liebert J., 1997, ApJ 491, 172
Sanduleak N., Pesch. P., 1984, ApJS 55, 517
Schmidt J.H.K., de Boer K.S., Heber U., Moehler S., 1996, A&A 306, L33
Schönberner D., 1993, In: Weinberger R., Acker A. (eds.) IAU Symposium No. 155: Planetary Nebulae, 415
Stetson P., 1991, AJ 102, 589
Sweigart A.V., 1987, ApJS 65, 95
Thejll P., Flynn C., Williamson R., Saffer R.A., 1997, A&A 317, 689
Tobin W., 1986, A&A 155, 326
Tody D., 1986, IRAF User Manual, NOAO Laboratory
Wallace P.T., 1992, Starlink User Note No. 67.17
Wesemael F., Fontaine G., Bergeron P., Lamontagne R., Green R.F., 1992, AJ 104, 203
Woltjer L., 1975, A&A 42, 109